J. Membrane Biol. 146, 177–191 (1995)

The Journal of
Membrane
Biology

The Permeation of Organic Cations through cAMP-gated Channels in Mammalian Olfactory Receptor Neurons

S. Balasubramanian[1], **J.W. Lynch**[2], **P.H. Barry**[1]

[1]School of Physiology and Pharmacology, University of New South Wales, Sydney, New South Wales, 2052, Australia
[2]Neurobiology Division, Garvan Institute of Medical Research, Darlinghurst, Sydney, New South Wales, 2010, Australia

Received: 17 November 1994/Revised: 15 March 1995

Abstract. The permeation of monovalent organic cations through adenosine 3′,5′-cyclic monophosphate-(cAMP) activated channels was studied by recording macroscopic currents in excised inside-out membrane patches from the dendritic knobs of isolated mammalian olfactory receptor neurons (ORNs). Current-voltage relations were measured when bathing solution Na^+ was replaced by monovalent organic cations. Permeability ratios relative to Na^+ ions were calculated from changes in reversal potentials. Some of the small organic cations tested included ammonium (NH_4^+), hydroxylammonium and formamidinium, with relative permeability ratios of 1.41, 2.3 and 1.01 respectively. The larger methylated and ethylated ammonium ions studied included: DMA (dimethylammonium), TMA (tetramethylammonium) and TEA (tetraethylammonium) and they all had permeability ratios larger than 0.09. Even large cations such as choline, arginine and tris(hydroxymethyl)aminomethane (Tris) were appreciably permeant through the cAMP-activated channel with permeability ratios ranging from 0.19 to 0.7. The size of the permeating cations, as assessed by molecular weight, was a good predictor of the permeability. The permeability sequence of the cAMP-activated channel in our study was $P_{NH4} > P_{Na} > P_{DMA} > P_{TMA} > P_{Choline} > P_{TEA}$. Higher permeability ratios of hydroxylammonium, arginine and tris(hydroxymethyl)aminomethane cannot be explained by ionic size alone. Our results indicate that: (i) cAMP-activated channels poorly select between monovalent cations; (ii) the pore dimension must be at least 6.5 × 6.5 Å, in order to allow TEA and Tris to permeate and (iii) molecular sieving must be an important mechanism for the permeation of large organic ions through the channels with specific ion binding playing a smaller role than in other structurally similar channels. In addition, the results clearly indicate that cyclic nucleotide-gated (CNG) channels in different cells are not the same, the olfactory CNG channel being different from that of the photoreceptors, particularly with respect to the permeation of large organic cations, which the ORN channels allow to permeate readily.

Key words: Olfactory receptor neuron — Dendritic knob — CyclicAMP — Cyclic nucleotide-gated channel — Monovalent organic cations

Introduction

The initial and most critical steps of olfactory signal transduction occur in the specialized cilia and the dendritic knob of the olfactory receptor neuron (ORN) (Firestein, Shephard & Werblin, 1990), where, on stimulation by odorants, a cascade of biochemical reactions occurs. This leads to the production of intracellular second messengers, of either adenosine 3′,5′-cyclic monophosphate (cAMP) or inositol 1,4,5,-trisphosphate (IP_3), alone or concurrently (Reed, 1992; Boekhoff et al., 1990; Ronnet, et al., 1993; Hatt & Ache, 1994). There is now clear evidence that many odorants activate the production of cAMP which directly activates a cation permeable channel, allowing a flux of cations to enter the cell (Nakamura & Gold, 1987). This cationic current depolarizes the membrane and drives the cell from its resting membrane potential towards the threshold for action potential generation. The cyclic nucleotide-gated (CNG) channel occupies a critical position in olfactory transduction and belongs to a family of ion channels directly activated by cyclic nucleotides, including the cGMP-activated channels in retinal cones (Haynes & Yau,

Correspondence to: P.H. Barry

1985), retinal rods (Fesenko, Kolesnikov & Lyubarsky, 1985), cells of the pineal gland (Dryer & Henderson, 1991), cochlear hair cells (Kolesnikov et al., 1991), cells of rabbit aorta (Biel et al., 1993) and mammalian sperm (Weyand et al., 1994). Some of these channels have been cloned and attempts have already been made to understand the structure-function relationship of these channels (for a review, *see* Kaupp, 1991). In this paper we wish to concentrate on the permeation properties of the mammalian olfactory CNG channels.

The selectivity of olfactory cyclic nucleotide-gated channels (CNG) to alkali monovalent cations has been studied in the rat and frog (Frings, Lynch & Lindemann, 1992) and it was found that the olfactory CNG channels are nonselective cation channels, discriminating poorly between alkali cations, having a pore with a single binding site (or at least single ion occupancy as suggested by the apparent lack of anomalous mole fraction behavior) and a conductance sequence which indicated that the binding site has a relatively high field strength. However, there has been no systemic study on the permeability of organic cations in the olfactory CNG channels. A previous report on CNG channels cloned from catfish olfactory neurons and expressed in *Xenopus* oocytes (Goulding, et al., 1993) has shown that the olfactory channel was permeable to trimethylammonium$^+$ whereas the cGMP-gated retinal channel, cloned from bovine retina was not. It also demonstrated the role of the H5 domain in determining the pore diameter and ion permeation through CNG channels. Preliminary data from that study suggested a larger pore diameter for the olfactory CNG channels. In our present study, we have investigated the permeation of many organic cations including methylated and ethylated ammonium derivatives and other large ions through the native CNG channels from the olfactory receptor neurons from adult female Wistar rats and we have found that indeed these channels must have a significantly larger pore dimension.

The aim of this paper was to investigate the permeability of monovalent organic cations as has been done in other ion channels (for a review, *see* Hille, 1992), and also to compare the permeation properties of CNG channels in the olfactory receptor neurons and retinal rods to organic cations (Picco & Menini, 1993) and the CNG channels with some voltage-gated and acetylcholine activated endplate channels.

We have shown from the results of our experiments that the CNG channel (activated by cAMP) from the dendritic knobs of mammalian olfactory receptor neurons is fairly nonselective amongst monovalent organic cations and is measurably permeable to all of the nine organic cations tested. The permeation properties also suggest that the channel is different from the photoreceptor channel and other voltage-gated channels and is comparable to the ACh-activated endplate channel (Dwyer, Adams & Hille, 1980). From the molecular dimensions of the large ions that permeate the channel, we can estimate that the open pore dimensions should be at least 6.5 Å × 6.5 Å in order to allow the cations TEA$^+$ and Tris$^+$ to pass through.

Preliminary results of this work have been published in abstract form (Balasubramanian, Lynch & Barry, 1994).

Materials and Methods

Cell Preparation

Enzymatically dissociated olfactory receptor neurons from adult female Wistar rats were obtained from olfactory epithelial tissue lining the septum and turbinates. Cell dissociation and isolation techniques are basically the same as described in detail previously (e.g., Lynch & Barry, 1991). In short, olfactory receptor neurons were enzymatically dissociated by incubating the olfactory epithelial tissue pieces in divalent cation-free Dulbecco's phosphate-buffered saline (DPBS) containing 0.2 mg/ml trypsin (Calbiochem, La Jolla, CA) for 27 min at 37°C. The dissociation was terminated by removing the dissociation solution and replacing it with 10 ml of General Mammalian Ringer's solution (GMR) to which 0.1 mg of trypsin inhibitor (Calbiochem, La Jolla, CA) had been added. After trituration with a wide bored pipette, 2 ml of the supernatant fluid with isolated cells were transferred to the recording chamber. The cells were allowed to settle down for about 30 min, after which they were continuously superfused with GMR throughout the period of experiment, which typically extended for about 3–5 hr. Olfactory receptor neurons were visually identified by their characteristic morphology and distinctive features including a spherical or ovoid soma (5–8 μm diameter), a single dendrite (~1 μm in diameter) arising from the soma and terminating in a swelling, the olfactory knob, of about 1–2 μm in diameter and bearing several fine cilia. The dissection and the experiments were performed at room temperature (20–22°C).

Electrophysiological Recording

The CNG channels (activated by cAMP) were studied in excised inside-out patches from the membranes of the dendritic knobs of isolated olfactory receptor neurons using standard patch clamp techniques (Hamill et al., 1981). Fire-polished patch pipettes with a tip diameter of about 0.2 μm and resistance of 10–15 MΩ were used to obtain gigaseals on the membrane. Channels were activated by the addition of 0.1 mM cAMP sodium salt (Sigma Chemical St. Louis, MI). Excised inside-out patches were obtained by brief air exposure. Currents were measured using an Axopatch-1D amplifier (Axon Instruments, Foster City, CA). The current signal was filtered at 2 kHz and digitized at a sampling interval of 0.1 msec and monitored online and stored on an IBM compatible computer running pCLAMP software (Axon Instruments, Foster City, CA), which was also used to control the D/A converter for generation of voltage clamp protocols and analysis of generated data.

Solutions and Perfusion System

The ion composition of the solution filling the patch pipette was the same in all the experiments and contained (in mM): NaCl 145, no added divalent salts, EGTA 2 and HEPES 10 titrated to pH 7.4 with Tris-base. The control solution bathing the cytoplasmic side of the membrane patch had the same composition. The test solutions in the bath were

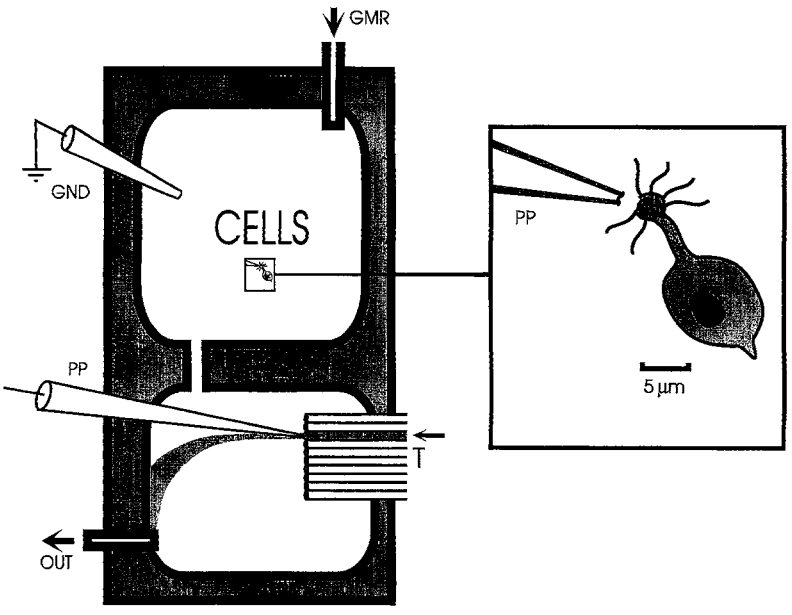

Fig. 1. The special multi-jet perfusion system used in our experiments and used for changing solutions across the patch of membrane spanning the tip of the patch-pipette, marked (PP). As already described, in Materials and Methods, the system consists of 2 compartments connected by a narrow channel. The compartment marked as "cells" served to store dissociated olfactory receptor neurons during the experiments and the cells were continuously superfused by General Mammalian Ringer's solution (GMR). On-cell patches were formed in this compartment. The figure in the inset (on the right), shows clearly how the membrane patches were obtained. The patch pipette (with a tip diameter of about 0.2 µm) was positioned against the knob membrane amidst the cilia and an inside-out patch was excised from it. The scale bar indicates about 5 µm. The second compartment was equipped with perfusion tubes (T) through which different solutions flowed. These bathed the patch of membrane spanning the tip of the patch pipette (PP), visually positioned in front of the outflow of the perfusion tubes. Solutions were changed rapidly and effectively by moving the perfusion tubes with the microscope stage on which the whole system was mounted.

similar except that the 145 mM NaCl was replaced by 145 mM of the salts of the test organic cation. Even with a contamination of Ca^{2+} in the range of 3 µM (which is what was found in similar solutions by Lynch and Lindemann, 1994), the addition of 2 mM EGTA will result in a free [Ca^{2+}] of less than 1 nM (Bers, 1982). The following salts were tested: NH_4Cl (from AnalaR, Victoria, Australia), hydroxylamine HCl, formamidine HCl, dimethylamine HCl, (all from TCI, Tokyo, Japan), tetramethylammonium chloride (from Merck, Germany), tetraethylammonium chloride, choline chloride, arginine HCl, and Tris HCl (all from Sigma Chemical, St. Louis, MO). All the test cations were tested at pH 7.4 except hydroxylamine, which, because of a pKa of 5.96, was tested at pH 5.8 to increase the concentration of the cationic species. The calculated concentration of the ionized species of hydroxylamine was 65 mM. Although lowering the pH further would have resulted in a higher ionized concentration, unfortunately the patches, which were already unstable in the presence of organic cations, were even more unstable at a lower pH (Picco & Menini, 1993).

A special multibarrel perfusion system was set up to enable us to change solutions very effectively and rapidly across the patch of membrane (Frings et al., 1992). The system consists of a sylgard chamber glued onto a standard microscope slide which was divided into 2 compartments connected by a narrow channel. One compartment served to store the cells during the experiment and in it the cells were continuously superfused by General Mammalian Ringer containing (in mM): NaCl 140, KCl 5, $CaCl_2$2, $MgCl_2$1, glucose 10,4-(2-hydroxy-ethyl)-1-piperazineethanesulfonic acid (HEPES) 10 (pH 7.4 with NaOH). On-cell patches were obtained among the cilia on the apical knobs of olfactory receptor neurons (*see* inset of Fig. 1) and excised in inside-out patch configurations by a brief air exposure. The other compartment was equipped with about 10 perfusion inlets allowing exposure of excised patches to different test solutions (*see* Fig. 1). After formation and excision of patches, the patch pipette was transferred through the intercompartmental channel and visually positioned in front of the outflow of the perfusion tubes through which the control and various test solutions flowed. The flow from any of the tubes could be started by just unclamping the feeding tube from the reservoir of solutions, in order to study and record the effect of an individual test solution. In all the experiments, complete recovery of current was checked by comparing the currents in symmetrical NaCl solutions, before and after each test solution.

Reversal Potentials and Permeability Ratios

The reversal (zero current) potential, E_{rev}, was determined under bi-ionic and symmetrical conditions. The solution filling the patch pipette at the extracellular side of the patch of membrane contained 145 mM NaCl and no added divalent ions, as described in the previous section. The fluid bathing the cytoplasmic side of the patch had the same composition, except that the 145 mM NaCl was replaced by 145 mM of the test salt. Step-voltage pulses, from a holding potential of 0 mV, increasing and decreasing in steps of 10 mV, or voltage ramps with 5 mV steps of 400 msec duration in both hyerpolarized and depolarized directions, were applied both in the presence and absence of 0.1 mM cAMP. cAMP activated currents were obtained from the difference of the recordings in the presence and absence of cAMP. Both voltage ramp and step methods yielded similar results. An example of the background currents in the absence of cAMP, which was subtracted to give the response due to cAMP alone, is shown in Fig. 2 *A* and *B*, in control sodium chloride and control hydroxylammonium hydrochloride solutions. In the absence of cAMP, the background conductances were in the ranges of 2–7 nS in control sodium chloride solution and typically 1–5 nS, in the control test solutions. In each case, the respective background traces were then subtracted from the traces with cAMP. The current traces in Figs. 5, 7 and 8, show the olfactory CNG currents in the presence of the respective cations with the appropriate background traces subtracted.

The average steady-state current was measured and plotted as a function of membrane potential. In all the experiments, the currents and potentials are represented with the usual sign convention: currents flowing from the intracellular side of the membrane patch (bath solution) to the extracellular side (pipette solution) are positive and are

plotted upwards. Reversal potentials were obtained by linear interpolation of the currents recorded in response to voltage steps around the reversal potential. Permeabilities relative to Na^+ (P_X/P_{Na}) were calculated by measuring the changes in the reversal potential, ΔE_{rev}, when the NaCl control solution was replaced by the test solution, using a modified form of the Goldman-Hodgkin-Katz potential equation for this simple bi-ionic condition (Hille, 1992):

$$P_X/P_{Na} = ([Na^+]/[X^+])\exp(-F\Delta E_{rev}/RT), \quad (1)$$

where R is the gas constant, F the Faraday constant, T the absolute temperature, $[X^+]$ and $[Na^+]$ the activity of the cation X^+ and Na^+ respectively. It should be noted that in the presence of permeant ions of only one sign and valency, the above equation is of a much more general validity than the model restrictions of the Goldman equation suggest (Barry & Gage, 1984). Since Tris base was used in all the solutions to keep the pH about 7.4, and $Tris^+$ turned out to be permeant, it became necessary to correct all the permeability measurements for the permeability of $Tris^+$. The equations used to do this and their derivation are given in the Appendix. In the resulting calculations, activities were substituted by concentrations, since the ionic strength of the solutions remained fairly constant. Liquid junction potentials were calculated for each solution (ranging from 3.6 to −3.7 mV), using the software program JPCalc (Barry, 1994; with additional mobility values from Ng & Barry, 1995) and the appropriate corrections to the membrane potential were applied.

Results

The primary aim of this paper was to investigate the permeation of some large organic cations through cAMP activated channels of mammalian olfactory receptor neurons and to compare our results with those from the cGMP-activated channel in the photoreceptors, in particular, and some of the other ligand-gated channels, in general.

Membrane patches excised from the dendritic knobs of the neurons in an inside-out configuration, on exposure to 0.1 mM cAMP in the absence of added divalent cations and in the presence of a control solution containing 145 mM of NaCl on both sides of the membrane, activated large currents. These were in the range of about 200 to 1200 pA. The single channel conductance of these channels, measured directly from separate single channel current traces, from the soma and dendritic membrane patches, varied from 2.4 pS to 10 pS. This indicated an activity of between 250–1500 cAMP activated channels in the patches from the dendritic knobs. The records of the actual currents passing through these channels were obtained from the difference of the recordings in the presence and absence of 0.1 mM cAMP (*see* Materials and Methods), as shown in Fig. 2*A*.

Although there have been other studies of the permeation of alkali cations through these channels already, some of our alkali cation (K^+, Cs^+, Li^+) permeation measurements have been included for comparison with the organic ions data. Our results ($P^+_{Na} = 1.0 > P^+_K = 0.84 > P^+_{Li} = 0.78 > P^+_{Cs} = 0.47$) agree reasonably well with the previous study ($P^+_{Na} = 1.0 > P^+_K = 0.81 > P^+_{Li} = 0.74 > P^+_{Rb} = 0.60 > P^+_{Cs} = 0.52$) of Frings et al. (1992).

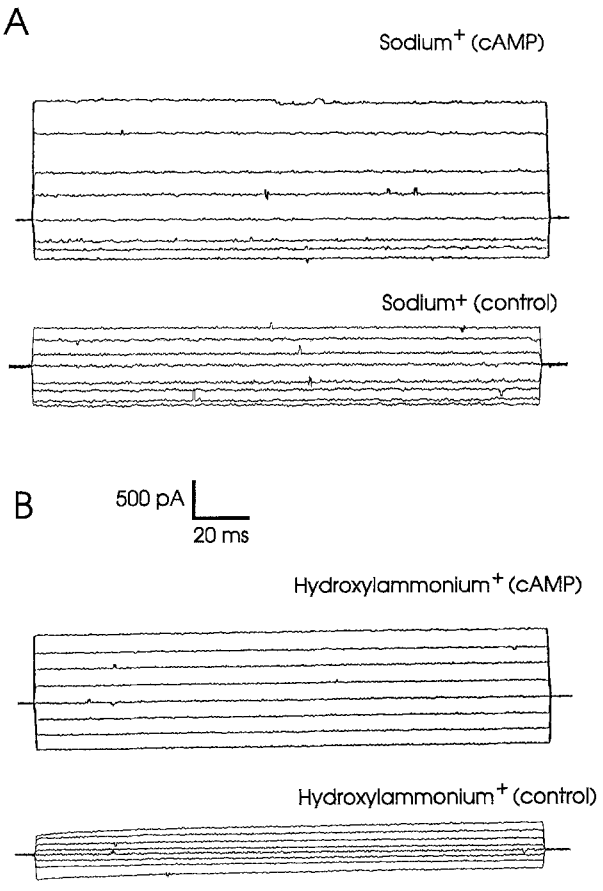

Fig. 2. CNG currents in patches from the dendritic knob of olfactory receptor neurons in the presence of hydroxylammonium$^+$ which has more than double the permeability relative to sodium$^+$. (*A*) and (*B*), top panels, show currents activated by 0.1 mM cAMP in the presence of sodium or hydroxylammonium at the (internal) cytoplasmic side of the membrane patches. It should be noted that the concentration of free hydroxylammonium$^+$ was less than half that of sodium (*see* text for details). Voltage pulses of 180 msec duration, from −80 to +70 mV in 10 mV steps, were given from a holding potential of 0 mV (only currents corresponding to 20 mV steps are shown). Each trace was obtained as the difference between the currents measured in the presence and absence of cAMP in the test solution. Lower panels of (*A*) and (*B*) show the typical background currents in the presence of control sodium and control hydroxylammonium solutions. The input conductance of the patch in the presence of sodium was 5–7 nS and in the presence of hydroxylammonium was 3–5 nS. The single scale bar applies to all 4 sets of traces.

Permeation of Ammonium$^+$ Derivatives of Small Dimensions and Formamidinium

The permeability of cAMP activated channels from dendritic knob of the olfactory receptor neurons was first investigated by replacing Na^+ with some ammonium derivatives of small dimensions *viz* ammonium (NH_4^+, mol.

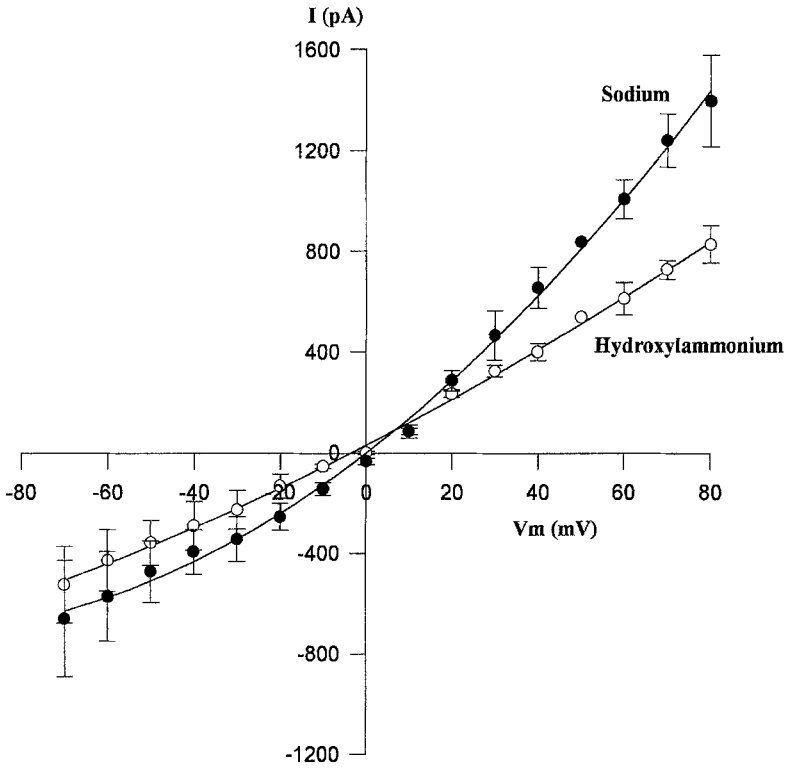

Fig. 3. Current-Voltage relations of olfactory CNG channels (activated by cAMP) when sodium$^+$ was replaced by hydroxylammonium$^+$. The data points represent the average of measurements from 4 patches. The error bars represent the SEM of the values and the curves represent the second order regression fits to the data. Since the ionized portion of hydroxylammonium available was only 65 mM compared to the value of 145 mM for sodium, the amplitude of the outward current is smaller. Using this concentration value for the test ions and the change in the reversal potential, the permeability of hydroxylammonium with respect to sodium can be shown to be 2.5 using Eq. (1) and after correction for the Tris cation added, it was found to be 2.3.

wt. 18.5) and hydroxylammonium$^+$ ($OHNH_3$, mol. wt. 34.0) and also formamidinium$^+$, an imidino group cation (NH_2:$CHNH_2^+$, mol. wt. 45.1). cAMP activated currents were recorded from the excised patches when the solution bathing the cytoplasmic side of the membrane contained Na^+ or various test organic cations. Currents were activated by 0.1 mM cAMP and voltage pulses from +80 to −70 mV in steps of 10 mV or voltage ramps of up to 100 mV in either directions, were applied to the patches. The average steady state current, I(pA), was plotted against the membrane potential, V_m, for the patches tested in Na^+ and each test cation solution and the resulting I-V relationships were plotted. The I-V plots shown were all tested for the individual test cation against the Na^+ response for the same patch and the results are the average of about 3–5 patches. The error bars indicate the SEM. The apparent permeability ratios relative to Na^+ were calculated with the Goldman-Hodgkin-Katz [Eq. (1)] by using the average values of the changes in reversal potential, and, where appropriate, taking into account the calculated ion concentration. Since $Tris^+$ was found to be permeant through these channels, (*see below*) all the permeability ratios given in the text have then been corrected using a finite value for P_{Tris}. Table 1 shows the uncorrected and corrected permeability ratios for the various ions tested, with the equations used for correcting these values (and their derivation) given in the Appendix.

When the NaCl bathing the cytoplasmic side of the patch was replaced by hydroxylammonium$^+$, which was the most permeant cation in our study, there was a change in the current amplitude (Fig. 2, *A* and *B*) as well as in the reversal potential. Hydroxylamine with a pK_a of 5.96 was the only test cation that had to be tested at pH 5.8, in order to effectively increase the ionized concentration of the ion for permeation (65 mM, at pH 5.8). The mean reversal potential change (ΔE_{rev}) obtained from the I-V of mean steady state current, I(pA), versus membrane potential, V_m, was only −3.1 mV (Fig. 3). However, when the actual concentration of hydroxylammonium$^+$ of 65 mM was substituted into Eq. (1), the deduced permeability ratio relative to Na^+ was as high as 2.5 and after correction for Tris cation permeability the relative permeability ratio was 2.3 (*see* Table 1). Since the lowered pH in Na^+ solution is shown to decrease only the amplitude of current through these channels and not alter the reversal potential (Frings et al., 1992), the permeability ratio calculated from the change in the reversal potential should be fairly accurate. Since the actual conductance of the channels in 65 mM Na^+ was not known, the conductance ratio g_X/g_{Na} was not calculated.

When ammonium chloride was used to replace NaCl in the bathing solution on the cytoplasmic side of the patch, the change in the reversal potential was obtained from plots of the mean steady-state current versus voltage (Fig. 4*A*) and the permeability ratio, P_{NH4}/P_{Na}, calculated from it. The mean reversal potential change in ammonium (ΔE_{rev}) was −8.3 mV (n = 4) giving a permeability of NH_4^+, relative to Na^+, of 1.41. At positive potentials, the average amplitude of the positive currents

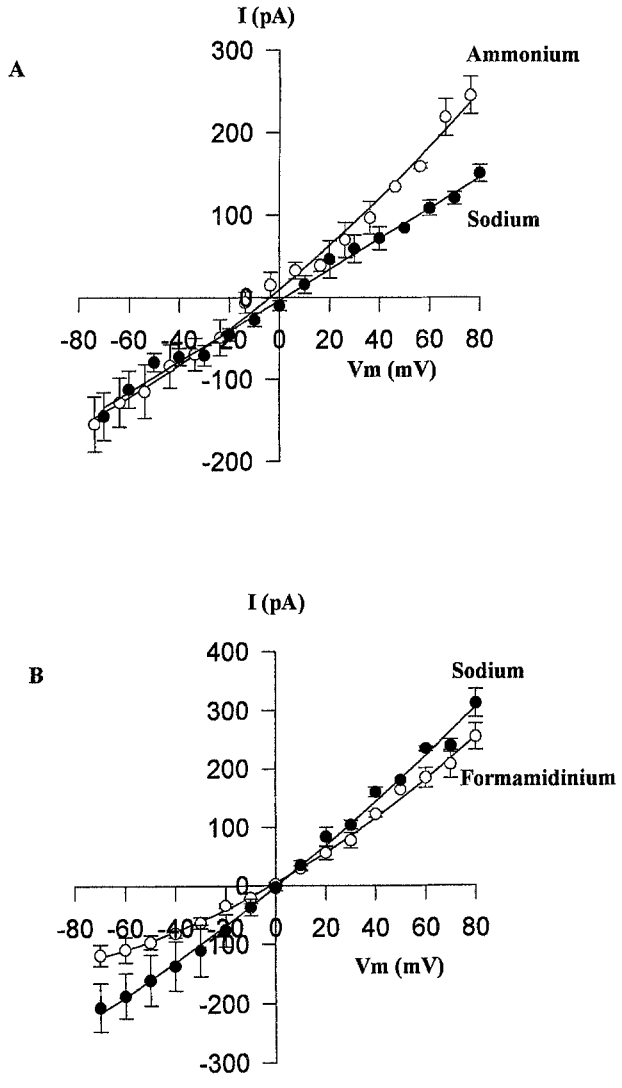

Fig. 4. Current-Voltage relations of olfactory CNG channels (activated by cAMP) when sodium was replaced by monovalent cations of small dimension on the cytoplasmic side of the dendritic knob patches. In each case the pipette solution contained Na^+. The data points represent the average of measurements from 4 patches. The error bars represent the SEM of the values and the continuous lines are second order regression fits to the data. (*A*) Current-voltage relations in bi-ionic and symmetrical solutions of ammonium and sodium. Note that the outward current in the presence of a bi-ionic solution with ammonium is more than that in symmetrical sodium solutions. (*B*) Current-Voltage relations in the presence of formamidinium (an ion of amidino group) and sodium. Note that formamidinium is as permeable as sodium through the CNG channel.

carried by the NH_4^+ ions was higher than that carried by the Na^+ ions, giving a conductance ratio, g^+_{NH4}/g^+_{Na}, of more than 1 (i.e., 1.85 at +70 mV). However at −70 mV, the conductance ratio was 0.97. (Table 1)

When formamidinium$^+$ (Form) replaced Na^+ ions, the reversal potential change was +0.7 mV (Fig. 4*B*). The relative permeability ratio was 1.01 and the conductance ratios g_{Form}/g_{Na} were 0.87 at +70 and 0.57 at −70 mV, respectively.

These results show clearly that the cAMP-gated channel is more permeable to NH_4^+ and hydroxylammonium$^+$ than to Na^+ itself and that formamidinium$^+$ is almost as permeant as Na^+ in the channel.

Permeation of Methylated and Ethylated Ammonium Derivatives (DMA, TMA and TEA)

The permeability of larger methylated and ethylated derivatives of ammonium was investigated in order to determine the selectivity of these ions and also to estimate the size of the pore of the channel from the dimensions of the largest cation that is able to permeate the channel. Outward currents are expected to be mainly carried by the test cation present at the cytoplasmic side of the membrane while inward currents are expected to be mainly carried by Na^+ ions at the extracellular side (pipette solution) of the membrane. Outward currents were recorded for all the three large cations studied (DMA, TMA and TEA; Figs. 5, 6, and 7), showing that the olfactory cAMP-activated channel is permeable to these large organic cations. Surprisingly, the amplitude of the inward current, was also markedly reduced in the presence of organic cations on the cytoplasmic side of the membrane. This is also a consistent observation by many other research groups concerned with organic cation permeation through various ligand-gated and transduction channels. In some experiments, a droop in the current was also observed (*see* Fig. 7*A*) and this has been attributed to adhesion of intracellular material to the surface membrane, causing restricted diffusion of ions (Zimmerman, Karpen & Baylor, 1988).

When dimethylammonium$^+$ (DMA, mol. wt. 46.1) replaced the Na^+ ions, the reversal potential change was +20.5 mV (Fig. 6) and the (corrected) calculated permeability ratio was 0.44. Tetramethylammonium (TMA, mol. wt. 74.6) was also permeant, as indicated by a change in the reversal potential of +27.3 mV, implying a permeability ratio of 0.31.

Tetraethylammonium (TEA, mol. wt. 130.7) was the least permeant ion in this study. In TEA solution there was a significant positive current at voltages more positive than +53 mV. From the mean change in the reversal potential of 53.8 mV, a relative permeability ratio of 0.09 was indicated. Table 1 gives an account of the change in the reversal potentials, permeability ratios and chord conductance ratios at +70 and −70 mV, for all the ions tested.

Since the permeability sequence of the large organic cations suggested that the channel distinguishes various permeant organic cations by their size, this seemed to imply a channel structure and size more related to the fairly nonselective cation channel of the endplate acti-

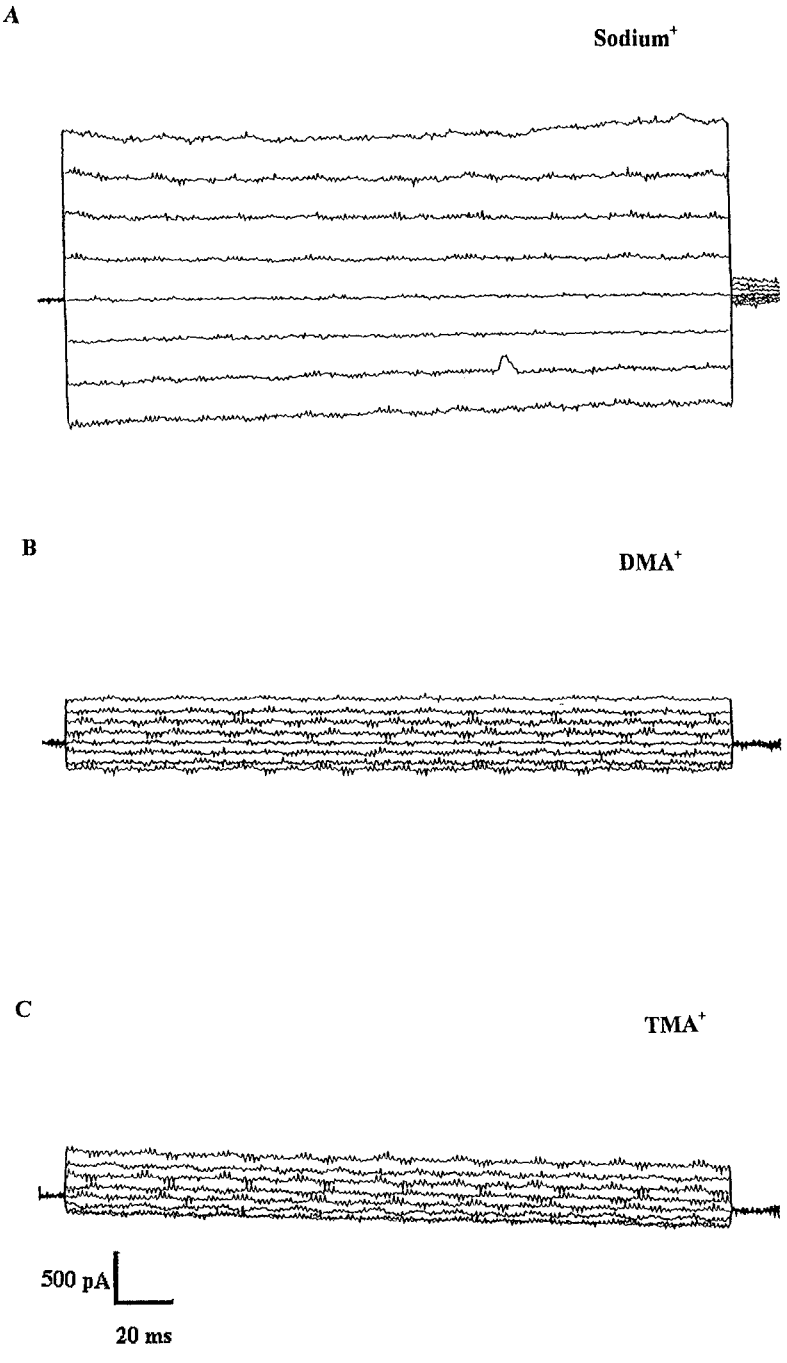

Fig. 5. (*A*)-(*C*) Olfactory CNG currents (cAMP-activated) in the presence of large methylated ammonium$^+$ compounds. Experiments were performed as described in the legend of Fig. 2, except that the duration of the voltage pulses was for 225 msec. Note that in the presence of DMA^+ and TMA^+ the inward currents were also greatly reduced and this has been attributed to pharmacological effects of these organic cations.

vated by acetylcholine (Dwyer et al., 1980). We, therefore, further studied the permeability of choline$^+$ and arginine$^+$ through these CNG channels.

Permeation of Choline and Arginine

When choline$^+$ (Chol, mol. wt. 104.2) was used to replace Na^+ ions, it was found that it was also permeant with a change in the reversal potential of +37.0 mV (Fig. 8), thus implying a permeability ratio of 0.19. Arginine$^+$ (Arg, mol. wt. 175.2) too was appreciably permeable through these channels with a change in the reversal potential of +10 mV (Fig. 9) and a relative permeability ratio of 0.66. It has been known that some large molecules like arginine are capable of assuming an elongated, spindle shape as they pass through channels and that this increases their permeability through them.

Having found that arginine which was barely permeant in the endplate channel ($P_{Arg}/P_{Na} < 0.014$) was clearly permeable in our olfactory CNG channel, we wanted to investigate the permeation of Tris, the base of which was used to titrate the pH of all test and control solutions used in the experiments.

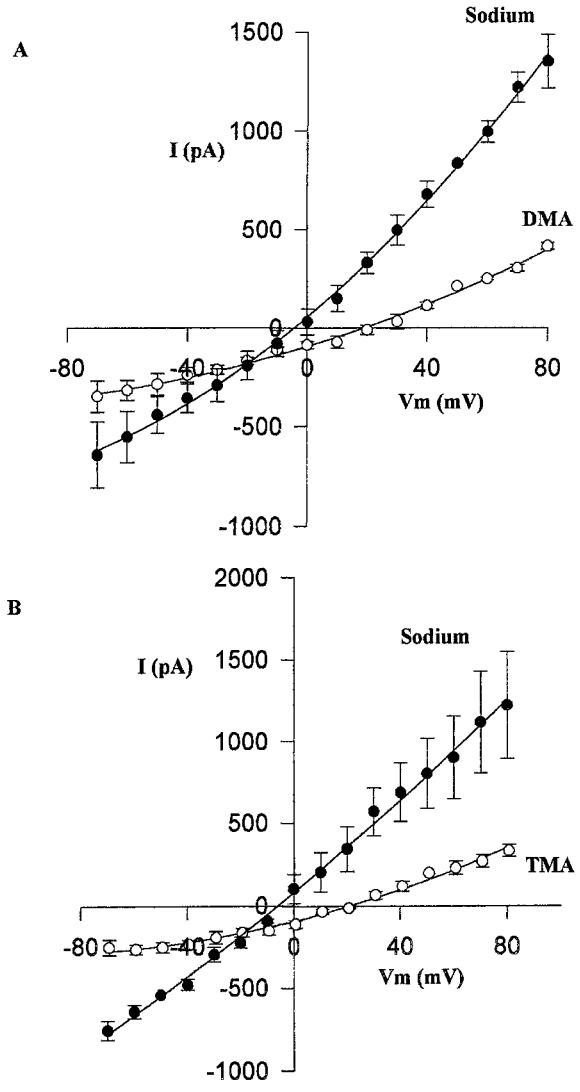

Fig. 6. Current-Voltage relations of the olfactory CNG channels (activated by cAMP) in the presence of symmetrical Na^+ and when Na^+ was replaced by DMA^+ (*A*) and TMA^+ (*B*) on the cytoplasmic side of the membrane patches from the dendritic knob. The data points represent the average of measurements from 4 patches. The error bars represent the SEM of the values and the continuous lines are the second order regression fits to the data points.

Permeation of Tris(Hydroxymethyl) Aminomethane

As foreshadowed already, Tris(hydroxymethyl)aminomethane$^+$ (Tris, mol. wt. 122.1) was found to be appreciably permeant. Tris had a permeability ratio of 0.65 relative to Na^+ and the change in its reversal potential was +10.8 mV (Fig. 10). This implied that corrections had to be applied to all our values of permeability ratios, allowing for the small but significant amounts of Tris base added to every other test solution in order to compensate for its finite permeability. Indeed this was very important in the case of the least permeable cation TEA and the permeability of TEA dropped from 0.12 to 0.09 after application of the correction (*see* Appendix).

Chord Conductance Ratios

Ionic selectivity of the organic cations was also measured in terms of the chord conductance ratio. Chord conductances were calculated at +70 and −70 mV from the currents and reversal potentials measured in the presence of permeant organic cations, normalized to the conductance in symmetrical Na^+ at the same potentials in the same patches and these values are listed in Table 1. Conductances at +70 mV were always from the outward currents and should have been mainly carried by test ions, whereas at −70 mV, they were from inward currents and should have been mainly carried by Na^+ ions. The ionic selectivity sequence obtained from the permeability ratios is different from that measured from chord conductance ratios, which is dependent on single channel conductance and the number of open channels.

Table 2 gives a comparison of the permeability ratios in the CNG channels of olfactory receptor neurons, retinal rod CNG channels, the ACh endplate channel and voltage-gated channels and Fig. 11 shows a graph of the plot of permeability ratios of the monovalent organic cations studied relative to Na^+ *vs.* the molecular weight of the respective organic cations in the CNG channels of the olfactory receptor neurons and the retinal rods (*see* discussion below).

Discussion

We have reported that the CNG channel of the olfactory neuron activated by cAMP in this study is permeable to at least nine monovalent organic cations including large molecules like TEA and Tris. Although there is increasing evidence for IP_3, as a second messenger in the transduction of some odorants, the CNG channel has been clearly shown to be the transduction channel for many odorants. It has been already shown that the CNG channels do not appreciably select among different monovalent alkali cations (Frings et al., 1992) and that divalent cations permeate the channel and block it and modulate its activity (Kramer & Siegalbaum, 1992; Kurahashi & Shibuya, 1990; Lynch & Lindemann, 1994; Zufall & Firestein, 1993). Knowledge of the ionic selectivity of this cyclic nucleotide-gated channel has been extended in this paper to a study of the permeation of a variety of monovalent organic cations including choline, arginine and Tris. The permeability of monovalent organic cations was found to be strongly determined by the size of the ion, and, in particular, our results suggest that the cAMP-activated channel of the olfactory receptors se-

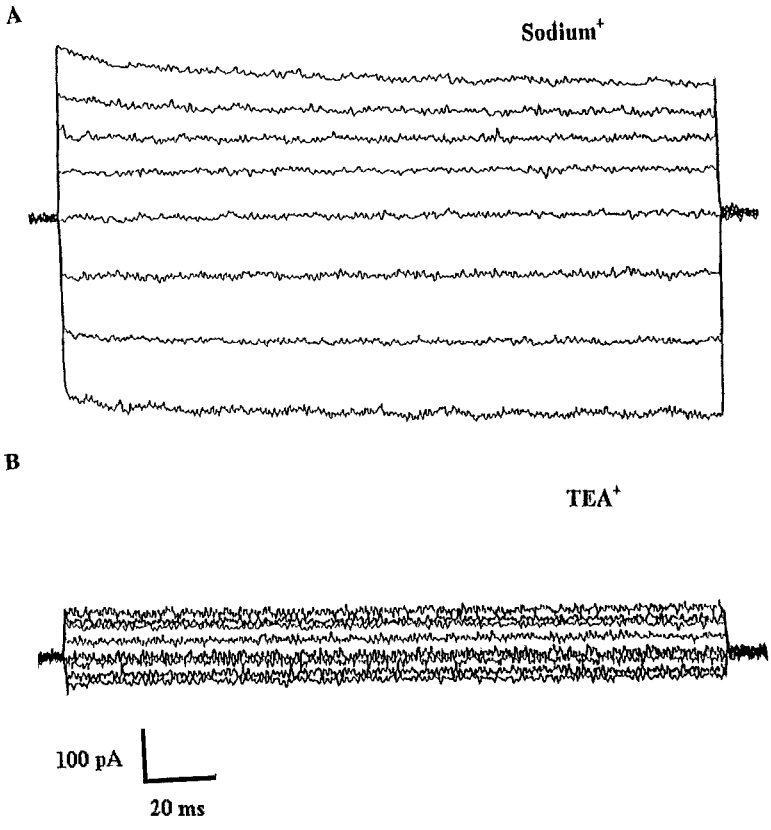

Fig. 7. (*A*) and (*B*) olfactory CNG currents (activated by cAMP) in the presence of symmetrical Na^+ and when it was replaced by TEA^+ on the cytoplasmic side of membrane patches from the dendritic knob. Experiments were performed as described in the legend of Fig. 2. The slight droop observed in the current traces in (*A*) was observed in some experiments and this has been attributed to hindered diffusion of ions due to the adherence of cytoplasmic material during patch excision (Zimmerman et al., 1988). Distinct outward currents are seen in the presence of TEA^+ which indicates that this large cation can permeate through the channel. (*C*) Current-Voltage relations of these channels in the presence of TEA^+ and Na^+. The data points represent the average of measurements from 3 patches. The error bars represent the SEM of the values and the continuous lines are polynomial regression fits to the data. The error bars are shown only if they are larger than the SEM.

lects large organic ions on the basis of geometric considerations.

Eisenman formulated an electrostatic model for selectivity among alkali monovalent cations based on the difference between the energy of dehydration of the cation permeating a channel and the energy of interaction with a binding site and initially he predicted 11 cation selectivity sequences for the 5 alkali cations (for a review, *see* Eisenman & Horn, 1983). The different selectivity sequences are caused by variations in the field strength of the site. The permeability selectivity sequence X (Na > K > Li > Rb > Cs) for the alkali cations through the CNG channel (this paper and Frings et al., 1992) suggests that it has a high field strength binding site, provided that the permeability is dominated by the equilibrium constant term. The analogous sequence X′ predicted by Eisenman et al. (1976) for the "main species" organic cations, also corresponds to a high field strength site and our study of organic cation permeation, with a selectivity sequence of hydroxylamine > ammo-

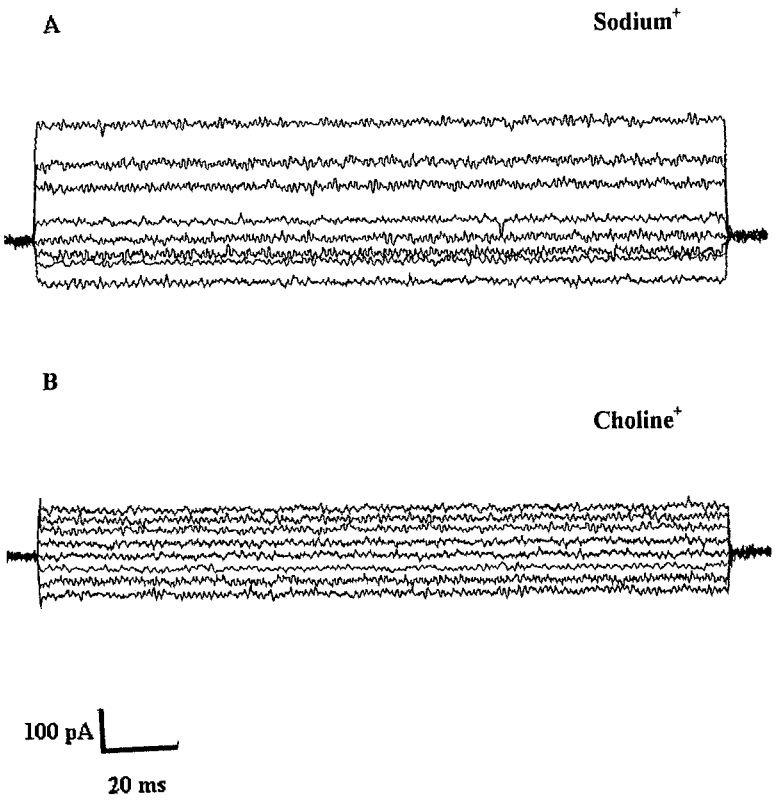

Fig. 8. (*A*) and (*B*) Olfactory CNG currents (activated by cAMP) in the presence of symmetrical Na^+ and when it was replaced by choline$^+$ on the cytoplasmic side of the dendritic knob membrane patches. Experiments were performed as described in the legends of Fig. 2. The recording of distinct outward current in the presence of choline$^+$ shows that this cation permeates through these channels. (*C*) Current-Voltage relations in the presence of choline$^+$ and Na^+. The data points represent the average of measurements from 3 patches. The error bars represent the SEM of the values and the continuous lines are polynomial regression fits to the data points.

nium > formamidinium is therefore, also, indicative of such a high field strength binding site sequence (Hille, 1972).

Pore Size

To obtain information about the narrowest region of the pore, the size and chemical nature of all the permeant ions were taken into account. Ions with amino or hydroxyl groups can form hydrogen bonds with oxygen containing groups and effectively reduce their size. But methylated ions which have a measurable permeability in our study, are not capable of forming hydrogen bonds (Hille, 1971). Hence the pore at its narrowest part must be at least as wide as the largest ion which it allows to pass through. Tris, with dimensions of 6.05 × 6.89 ×

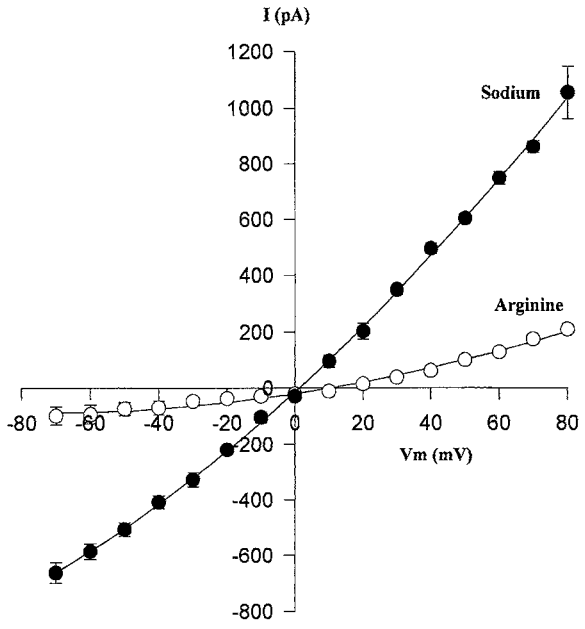

Fig. 9. Current-Voltage relations for the olfactory CNG channels when arginine$^+$ was used to replace Na^+ on the cytoplasmic side of the dendritic knob membrane patches. The graph clearly shows that this large cation is measurably permeant through the cAMP-activated channel in this study. The data points represent the average of measurements from 3 patches. The error bars are the SEM of the values and the continuous lines are polynomial regression fits to the data points.

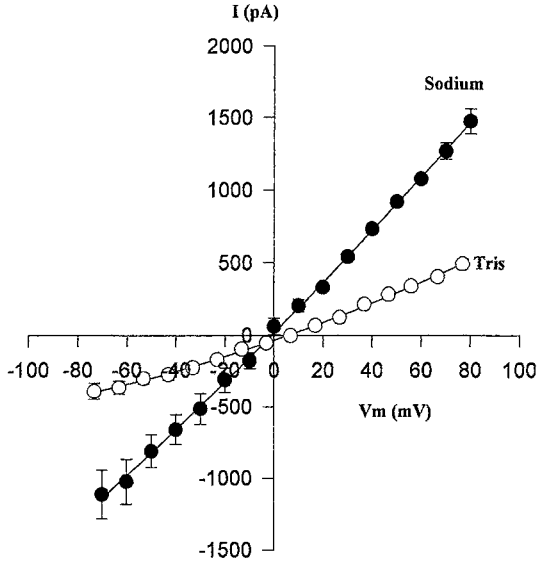

Fig. 10. Current-Voltage relations of olfactory CNG channels when Tris$^+$ replaced Na^+ on the cytoplasmic side of the dendritic knob membrane patches. It is very clear that this cation is permeable through the channel. The data points represent the average of measurements from 6 patches. The error bars represent the SEM of the values and the continuous lines are polynomial regression fits to the data points.

7.71 Å (Huang, Catterall and Ehrenstein, 1978) as well as TEA, with a diameter of 6.3–6.5 Å (calculated from Pauling, 1960; Huang et al., 1978; McCleskey & Almers, 1985), are permeant through the channel and hence, the

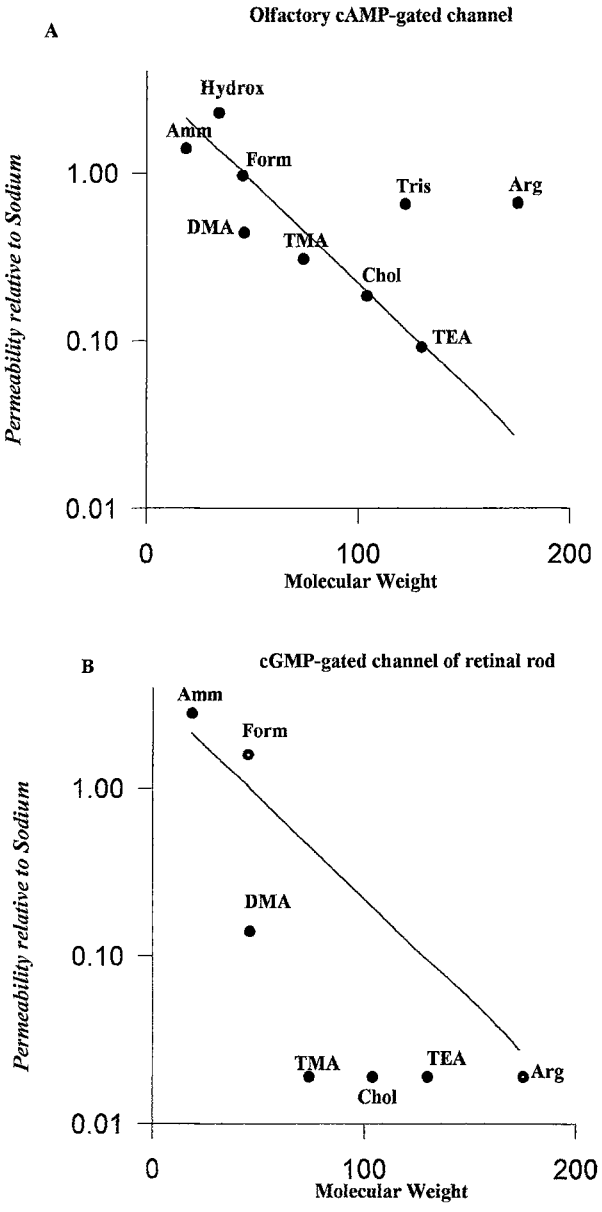

Fig. 11. A graph showing the relationship between the relative permeability ratios (on a log scale) of the monovalent organic cations studied relative to sodium and the molecular weight of the ions. (*A*) data from this study on CNG channels of the olfactory system (activated by cAMP) and (*B*) data from the study on CNG channels from retinal rods, activated by cGMP (Picco & Menini, 1993). A comparison of the two graphs makes it very clear that the olfactory CNG channel is the larger channel, being permeable to the large methylated and ethylated ammonium ions and also to choline and arginine, which are almost impermeant through the photoreceptor CNG channels. The curve drawn is the function 3.6 exp(−0.028 · mol wt), from Dwyer et al. (1980), for the ACh channel, merely used to suggest the trend of the data.

pore size should be at least 6.5 × 6.5 Å at its narrowest region. On geometric grounds, such a pore could also be permeable to many larger molecules, provided that they were capable of assuming an elongated, spindle shape, as arginine is (Dwyer et al., 1980).

Table 1. Reversal potentials, permeability and chord conductance ratios for olfactory CNG channels from dendritic knob patches

X_i^+	ΔE_{rev} (mV)	n	$[X^+]_i$ (mM)	$[Tris^+]_i^X$ (mM)	P_X/P_{Na}*	P_X/P_{Na}	g_X^+/g_{Na}^+ +70 mV	g_X^-/g_{Na}^- −70 mV
Ammonium	−8.3 ± 2.6	4	145	13	1.39	1.41	1.85	0.97
Hydroxylammonium	−3.1 ± 2.8	4	65	37.5	2.52	2.29		
Formamidinium	+0.7 ± 0.3	4	145	7.0	0.98	1.01	0.87	0.57
DMA	+20.5 ± 2.2	4	145	8.0	0.45	0.44	0.35	0.42
TMA	+27.3 ± 2.9	4	145	12.0	0.34	0.31	0.42	0.23
TEA	+53.8 ± 0.1	3	145	8.0	0.12	0.09	0.44	0.28
Choline	+37.0 ± 0.1	3	145	13.0	0.23	0.19	0.83	0.58
Arginine	+10.1 ± 0.1	3	145	11.0	0.67	0.66	0.24	0.13
Tris	+10.9 ± 1.2	6	145	12.9		0.65	0.41	0.28

X_i^+ refers to the test cation, ΔE_{rev} the average change of reversal potential, n the number of patches studied, $[X^+]_i$ the cation concentration, $[Tris^+]_i^X$ refers to the Tris cation added to the internal solution, P_X/P_{Na}* the uncorrected permeability ratio calculated using Eq. (1), P_X/P_{Na} the corrected permeability ratio, corrected for the presence of the permeant Tris cation (*see* Appendix, using $[Tris^+]_i^{Na}$ = 12.9 mM and $[Tris^+]_i^X$ as given above). The ratios, g_X^+/g_{Na}^+ and g_X^-/g_{Na}^- are the chord conductance ratios at +70 mV and −70 mV respectively. All the mean values are shown as ± SEM.

Permeability and Conductance Ratios

Permeability and conductance ratios are two different ways of measuring selectivity and, in general, they do not give similar values (Hille, 1992). Permeability ratios are easier to interpret and they are independent of the number of open channels, while macroscopic conductance is dependent on both the single channel conductance and the number of open channels. Both of these parameters can be modified by the presence of different ions, especially the organic cations which can also have a pharmacological blocking effect.

An analysis of the *inward* Na^+ conductances indicates that they were reduced by the presence of various cations at the *cytoplasmic* side of the membrane patch. If it is assumed that these cations do not alter the number of open channels, then the smaller Na^+ conductance must be due to a pharmacological effect of these organic cations (Hille, 1971). As already suggested by Menini (1990) for the CNG channels of the photoreceptors, the structure of the CNG channels in olfactory receptor neurons may also consist of a narrow portion, behaving as a one ion pore, and a large vestibule at the cytoplasmic side with weakly voltage dependent binding sites, which can be occupied by both permeant and impermeant cations. However, by analogy with other ligand-gated ion channels (e.g., Fatima-Shad & Barry, 1993) it seems more likely that the channels behave as a multi-ion pore.

Comparison with Other Channels

Since the olfactory CNG channel has extensive amino acid sequence identity with the photoreceptor CNG channel (Kaupp, 1991), it is reasonable to compare its permeation properties with those of the CNG channel of retinal rods (Picco & Menini, 1993). Interestingly, we have found that the olfactory channel is different from the retinal channels. From our Fig. 11, which shows the graph of permeability ratio of various organic cations *vs.* their molecular weight for our CNG olfactory neuronal channels and the CNG channels of retinal rods (Picco & Menini, 1993), it may clearly be seen that the olfactory channels are more permeable to methylated and ethylated ammonium ions as well as being permeable to other large cations like choline, arginine and Tris. In contrast, the largest methylated ammonium ion permeable through the photoreceptor channels is DMA with cations like choline and arginine being almost impermeant (P_{Chol}/P_{Na},$P_{Arg}/P_{Na} < 0.019$). Our study also shows that our olfactory CNG channels have a larger pore and that ion permeation through these channels is largely determined by the size of the ions (molecular sieving) whereas specific ion binding seems to play a more dominant role in the retinal channels. It has already been shown that structurally the CNG channels are related to the superfamily of voltage-gated Na^+, K^+, and Ca^{2+} channels and belong to the same class of channels (Jan & Jan, 1990; Kaupp, 1991; Goulding, et al., 1992). However, the results of our experiments show that functionally the olfactory CNG channel is very different from voltage-dependent Na^+ channels, which exclude methylamine (Hille, 1971), and the delayed rectifier K^+ channels (Hille, 1973), where NH_4^+ is the only organic cation known to be permeant. Instead, our study shows that the olfactory CNG channel has much more in common with the relatively nonselective endplate nicotinic ACh channel through which large methylated ammonium ions, choline, Tris and arginine are permeable (Dwyer et al., 1980) and the Ca^{2+} channel of skeletal muscle, which is permeable to large methylated ammonium ions in the absence of divalent cations (McCleskey & Almers, 1985). Table 2 shows a comparison of permeability ratios in olfactory CNG channels and with such ratios in other channels. A comparison between the estimated minimum pore diameters of these channels shows that the olfactory CNG channel (6.5 × 6.5 Å) is larger than

Table 2. Comparison of permeability ratios in the CNG channels of olfactory receptor neurons, retinal rod CNG channels and in other channels

Cation$^+$/channel	Olf	Ret	ACh	Na^+	K^+	Ca^{++}
Hydroxylammonium	2.29	5.92	1.92	0.94	<0.025	
Ammonium	1.41	2.80	1.79	0.16	0.13	1.50
Formamidinium	1.01	1.00	1.58	0.14	<0.020	
Dimethylammonium	0.44	0.14	0.87	<0.007		0.67
Tetramethylammonium	0.31	<0.019		<0.005		0.055
Tetraethylammonium	0.09	<0.019		<0.008		
Choline	0.19	<0.019	0.13	<0.007		
Arginine	0.66		<0.014			
Tris	0.65		0.018			
Na	1.0	1.0	1.0	1.0	0.01	1.0
K	0.84	0.98	1.11	0.086	1.0	0.8
Li	0.78	1.14	0.87	0.93	<0.018	
Rb	0.60*	0.84	1.30	<0.012	0.91	0.6
Cs	0.47	0.58	1.42	<0.013	<0.077	0.35

Column 1 lists the cations tested. Column 2 (Olf) shows the permeability ratios relative to Na^+ (P_x/P_{Na}) for the CNG channel of the olfactory receptor neuron (activated by cAMP) from the experiments described in this paper and *from Frings et al. (1992). Column 3 (Ret) shows the P_x/P_{Na} for the CNG channel of retinal rods (activated by cGMP; Picco & Menini, 1993 and Menini, 1990). Column 4 (ACh) shows P_x/P_{Na} for the ACh endplate channel (Adams, Dwyer & Hille, 1980; Dwyer et al., 1980). Column 5 (Na^+) shows the P_x/P_{Na} for the sodium channel of the node of Ranvier (Hille, 1971, 1972). Column 6 (K^+) shows permeability ratios relative to K^+ for the potassium channel of the node of Ranvier (Hille, 1973). Column 7 (Ca^{2+}) shows P_x/P_{Na} for organic cations in the calcium channel of skeletal muscle (McCleskey & Almers, 1985) and for alkali cations in the calcium channel of mouse neoplastic B lymphocytes (Fukushima & Hagiwara, 1985).

the retinal rod CNG channel (3.8 × 5.0 Å; Picco & Menini, 1993); the Na^+ channel (3.0 × 5.0 Å; Hille, 1971); the K^+ channel (3.0 Å diameter; Hille, 1973), and the Ca^{2+} channel of skeletal muscle (5.5 × 5.5 Å square; McCleskey & Almers, 1985) but that it is similar in size to the ACh endplate channel (6.5 × 6.5 Å; Dwyer et al., 1980).

The role of cations in olfactory reception has been studied and it has been shown that the olfactory response can be elicited by a variety of ions including choline and Tris (Yoshii & Kurihara, 1983). The CNG conductance was not discovered in the ciliary membrane of the olfactory receptor cells at that time, and the authors concluded that the receptor potential generated in the presence of the large organic cations was due to a change in the interfacial potential at the outer surface of the microvilli membrane. However, choline was not found to be permeable through the CNG channels in some of the species like newt (Kurahashi, 1990) and *Xenopus laevis* olfactory receptor neurons (Schild & Lischka, 1994). In our study, choline was found to be clearly permeable through the mammalian olfactory CNG channel with a small but definite permeability of 0.19 relative to sodium. The difference between the above results and ours may either be due to the presence of high amounts of divalent ions in these studies and/or to species differences. Our present experiments demonstrate very clear permeation of large organic cations through the CNG channels in membrane patches from the olfactory dendritic knob and this indicates that olfactory receptor neurons are capable of generating receptor potentials in the presence of these various ions as they permeate the CNG channels. Thus, care must be exercised in the interpretation of data obtained using large, supposedly impermeant, ions.

Under physiological conditions, the relative nonselectivity and large pore size of the transduction channel may be implicated in the speed and efficacy of signal transduction, by allowing various ions available in the immediate environment to enter the cells and depolarize them, upon odorant stimulation, provided the higher calcium concentration has not changed the selectivity of these channels significantly. It has already been shown that the opening of a single channel can elicit an action potential in these very small neurons with such a high input resistance (Lynch & Barry, 1989), and our results show that this CNG channel (activated by cAMP) with its large pore size and relative nonselectivity can allow various cations to enter the cell and initiate a response on stimulation by odorants.

This work was supported by the Australian Research Council of Australia.

References

Adams, D.J., Dwyer, T.M., Hille, B. 1980. The permeability of endplate channels to monovalent and divalent metal cations. *J. Gen. Physiol.* **75**:493–510

Balasubramanian, S., Lynch, J.W., Barry, P.H. 1994. Permeation of organic cations through cAMP-gated channels in mammalian olfactory receptor neurons. *Proc. Aust. Physiol. Pharmacol. Soc.* **25:**125P

Barry, P.H. 1994. JPCalc, a software package for calculating liquid junction potential corrections in patch-clamp, intracellular, epithelial and bilayer measurements and for correcting junction potential measurements. *J. Neurosci. Methods* **51:**107–116

Barry, P.H., Gage, P.W. 1984. Ionic selectivity of channels at the end plate. *Curr. Top. Membr. Transp.* **21:**1–51

Bers, D.M. 1982. A simple method for the accurate determination of free [Ca^{2+}] in Ca-EGTA solutions. *Am. J. Physiol.* **242:**C404–408

Biel, M., Altenhofen, W., Hullin, R., Ludwig, J., Freichel, M., Flockerzi, V., Dascal, N., Kaupp, U.B., Hofmann, F. 1993. Primary structure and functional expression of a cyclic nucleotide-gated channel from rabbit aorta. *FEBS Lett.* **320:**134–138

Boekhoff, I., Tareilus, E., Strotmann, J., Breer, H. 1990. Rapid activation of alternate second messenger pathways in olfactory cilia from rats by different odorants. *EMBO J.* **9:**2453–2458

Dryer, S.E., Henderson, D. 1991. A cyclic GMP-activated channel in dissociated cells of the chick pineal gland. *Nature* **353:**756–758

Dwyer, T.M., Adams, D.J., Hille, B. 1980. The permeability of the endplate channel to organic cations in frog muscle. *J. Gen. Physiol.* **75:**469–492

Eisenman, G., Horn, R. 1983. Ionic selectivity revisited: the role of kinetic and equilibrium processes in ionic permeation through channels. *J. Membrane Biol.* **76:**197–225

Eisenman, G., Krasne, S., Ciani, S. 1976. Further studies on ion selectivity. *In:* Ion Selective Electrodes and Enzyme Electrodes in Medicine and Biology, M. Kessler, L. Clark, D. Lubbers, I. Silver, W. Simon, editors. pp. 3–22. Urban and Schwarzenberg, Munich

Fatima-Shad, K., Barry, P.H. 1993. Anion permeabilities in GABA- and glycine-gated channels of mammalian cultured hippocampal neurons. *Proc. R. Soc. Lond. B* **253:**69–75

Fesenko, E.E., Kolesnikov, S.S., Lyubarsky, A.L. 1985. Induction by cGMP of cationic conductance in plasma membrane of retinal rod outer segment. *Nature* **313:**310–313

Firestein, S., Shepherd, G.M., Werblin, F.S. 1990. Time course of the membrane current underlying sensory transduction in salamander olfactory receptor neurons. *J. Physiol.* **430:**135–158

Frings, S., Lynch, J.W., Lindemann, B. 1992. Properties of cyclic nucleotide-gated channels mediating olfactory transduction: activation, selectivity, and blockage. *J. Gen. Physiol.* **100:**45–67

Fukushima, Y., Hagiwara, S. 1985. Currents carried by monovalent cations through calcium channels in mouse neoplastic B lymphocytes. *J. Physiol.* **358:**255–284

Goulding, E.H., Ngai, J., Kramer, R.H., Colicos, S., Axel, R., Siegalbaum, S.A., Chess, A. 1992. Molecular cloning and single-channel properties of the cyclic nucleotide-gated channel from catfish olfactory neurons. *Neuron* **8:**45–58

Goulding, E.H., Tibbs, G.R., Liu, D., Siegalbaum, S.A. 1993. Role of H5 domain in determining the pore diameter and ion permeation through cyclic nucleotide-gated channels. *Nature* **364:**61–64

Hamill, O.P., Marty, A., Neher, E., Sakmann, B., Sigworth, F.J. 1981. Improved patch-clamp techniques for high resolution current recording from cells and cell-free membrane patches. *Pfluegers. Arch. Eur. J. Physiol.* **391:**85–100

Hatt, H., Ache, B.W. 1994. Cyclic nucleotide- and inositol phosphate-gated ion channels in lobster olfactory receptor neurons. *Proc. Natl. Acad. Sci. USA* **91:**6264–6268

Haynes, L.W., Yau, K.W. 1985. Cyclic GMP-sensitive conductance in outer segment membrane of catfish cones. *Nature* **317:**61–64

Hille, B. 1971. The permeability of the sodium channel to organic cations in myelinated nerve. *J. Gen. Physiol.* **58:**599–619

Hille, B. 1972. The permeability of the sodium channel to metal cations in myelinated nerve. *J. Gen. Physiol.* **59:**637–658

Hille, B. 1973. Potassium channels in myelinated nerve: Selective permeability to small cations. *J. Gen. Physiol.* **61:**669–686

Hille, B. 1992. *In:* Ionic Channels of Excitable Membranes. Sinauer Associates, Sunderland, MA

Huang, L.M., Catterall, W.A., Ehrenstein, G. 1978. Selectivity of cations and nonelectrolytes for acetylcholine-activated channels in cultured muscle cells. *J. Gen. Physiol.* **71:**397–410

Jan, L.Y., Jan, Y.N. 1990. A superfamily of ion channels. *Nature* **345:**672

Kaupp, U.B. 1991. The cyclic nucleotide-gated channels of vertebrate photoreceptors and olfactory epithelium. *Trends in Neurosciences* **14:**150–157

Kolesnikov, S.S., Rebrik, T.I., Zhainazarov, A.B., Tavartkiladze, G.A., Kalamkarov, G.R. 1991. A cyclic-AMP-gated conductance in cochlear hair cells. *FEBS Lett.* **290:**167–170

Kramer, R.H., Siegalbaum, S.A. 1992. Intracellular Ca^{2+} regulates the sensitivity of cyclic nucleotide-gated channels in olfactory receptor neurons. *Neuron* **9:**897–906

Kurahashi, T. 1990. The response induced by intracellular cyclic AMP in isolated olfactory receptor cells of the newt. *J. Physiol.* **430:**355–371

Kurahashi, T., Shibuya, T. 1990. Ca^{2+}-dependent adaptive properties in the solitary olfactory receptor cell of the newt. *Brain Res.* **515:**61–268

Lynch, J.W., Barry, P.H. 1989. Action potentials initiated by single channels opening in a small neuron (rat olfactory receptor). *Biophys. J.* **55:**755–768

Lynch, J.W., Barry, P.H. 1991. Properties of transient K^+ currents and underlying single K^+ channels in rat olfactory receptor neurons. *J. Gen. Physiol.* **97:**1043–1072

Lynch, J.W., Lindemann, B. 1994. Cyclic nucleotide-gated channels of rat olfactory receptor cells: divalent cations control the sensitivity to cAMP. *J. Gen. Physiol.* **103:**87–106

McCleskey, E.W., Almers, W. 1985. The Ca channel in skeletal muscle is a large pore. *Proc. Natl. Acad. Sci. USA* **82:**7149–7153

Menini, A. 1990. Currents carried by monovalent cations through cyclic GMP-activated channels in excised patches from salamandar rods. *J. Physiol.* **424:**167–185

Nakamura, T., Gold, G.H. 1987. A cyclic nucleotide-gated conductance in olfactory receptor cilia. *Nature* **325:**442–444

Ng, B., Barry, P.H. 1995. The measurement of ionic mobilities of certain less common organic ions needed for junction potential corrections in electrophysiology. *J. Neurosci. Methods* **56:**37–41

Pauling, L. 1960. Nature of the Chemical Bond. Cornell University Press, Ithaca, NY

Picco, C., Menini, A. 1993. The permeability of the cGMP-activated channel to organic cations in retinal rods of the tiger salamander. *J. Physiol.* **460:**741–758

Reed, R.R. 1992. Signaling pathways in odorant detection. *Neuron* **8:**205–209

Ronnet, G.V., Cho, H., Hester, L.D., Wood, S.F., Snyder, S.H. 1993. Odorants differentially enhance phosphoinositide turnover and adenyl cyclase in olfactory receptor neuronal cultures. *J. Neurosci.* **13:**1751–1758

Schild, D., Lischka, F.W. 1994. Amiloride-insensitive cation conductance in *Xenopus laevis* olfactory neurons: a combined patch clamp and calcium imaging analysis. *Biophys. J.* **66:**299–304

Weyand, I., Godde, M., Frings, S., Weiner, J., Muller, F., Altenhofen, W., Hatt, H., Kaupp, U.B. 1994. Cloning and functional expression of a cyclic nucleotide-gated channel from mammalian sperm. *Nature* **368:**859–863

Yoshii, K., Kurihara, K. 1983. Role of cations in olfactory reception. *Brain Res.* **274:**239–248

Zimmerman, A.L., Karpen, J.W., Baylor, D.A. 1988. Hindered diffusion in excised membrane patches from retinal rod outer segments. *Biophys. J.* **54:**351–355

Zufall, F., Firestein, S. 1993. Divalent cations block the cyclic nucleotide-gated channel of olfactory receptor neurons. *J. Neurophysiol.* **69:**1758–1768

Appendix

Bi-ionic Reversal Potential Correction for Permeant Tris Ions

P.H. Barry

This appendix derives the permeability corrections for bi-ionic solutions across a patch of membrane in the presence of a permeant species (e.g., Tris) present in all the solutions. It will also be considered that the ionic channels are essentially only permeable to cations, as in the case of the CNG channels in this paper, and that the solution on one of the sides of the patch remains constant. In such bi-ionic measurements with inside-out patches, the outside membrane interface facing the pipette solution will be considered to remain common. In this paper, Tris base had been used in all the solutions to maintain the pH close to 7.4, and in these CNG channels Tris had turned out to be permeant, thus making it necessary to correct for the permeability of Tris in all the reversal potential measurements. The equation for applying such corrections will now be derived. Since these channels are essentially anion impermeant, the generalized reversal (null) potential equation (e.g., Barry & Gage, 1984), has the same form as the Goldman-Hodgkin-Katz equation, but is of much more general application than is suggested by the assumptions of the Goldman-Hodgkin-Katz equation.

For example, for measurements with mainly Na in the bathing solution, $[Na]_i$ and in the pipette, $[Na]_o$, the reversal potential, E_{rev}^{Na}, which should be close to zero will be given by:

$$E_{rev}^{Na} = (RT/F)\ 1n[(P_{Na}[Na]_o + P_{Tris}[Tris]_o)/(P_{Na}[Na]_i + P_{Tris}[Tris]_i^{Na})] \quad (A1)$$

where subscripts o and i refer to the outside membrane surface (pipette) and inside membrane surface (bathing solution) concentrations respectively, P_{Na} and P_{Tris} represent the relative Na and Tris permeabilities, $[Tris]_i^{Na}$ represents the concentration of Tris in the Na solution and R, T and F have their usual significance.

When the bathing solution cation is changed from Na to X, the new reversal potential will be given by:

$$E_{rev}^{X} = (RT/F) \cdot 1n[(P_{Na}[Na]_o + P_{Tris}[Tris]_o)/(P_X[X]_i + P_{Tris}[Tris]_i^X)] \quad (A2)$$

where $[Tris]_i^X$ represents the concentration of Tris in the X solution, which, in general, need not be the same as $[Tris]_i^{Na}$. Subtracting Eq. (A1) from Eq. (A2), the difference, $E_{rev}^{X} - E_{rev}^{Na} \equiv \Delta E_{rev}^{X/Na}$, will be given by:

$$E_{rev}^{X/Na} = (RT/F) \cdot 1n[(P_{Na}[Na]_i + P_{Tris}[Tris]_i^{Na})/(P_X[X]_i + P_{Tris}[Tris]_i^X)] \quad (A3)$$

and

$$\alpha \equiv \exp(-\Delta E_{rev}^{X/Na}\ F/RT) = (P_X[X]_i + P_{Tris}[Tris]_i^X)/(P_{Na}[Na]_i + P_{Tris}[Tris]_i^{Na}) \quad (A4)$$

Dividing both numerator and denominator of Eq. (A4) by $P_{Na}[Na]_i$ results in:

$$\alpha = [(P_X/P_{Na}) \cdot ([X]_i/[Na]_i) + (P_{Tris}/P_{Na}) \cdot ([Tris]_i^X/[Na]_i)]/(1 + \beta_2) \quad (A5)$$

where

$$\beta_2 \equiv (P_{Tris}/P_{Na}) \cdot ([Tris]_i^{Na}/[Na]_i)$$

Now, if it were assumed that $P_{Tris} = 0$, then the apparent permeability ratio $(P_X/P_{Na})^*$ would be given by:

$$\alpha = (P_X/P_{Na})^*([X]_i/[Na]_i) \quad (A6)$$

Expanding Eq. (A6), it may be shown that:

$$(P_X/P_{Na})^* = ([Na]_i/[X]_i)\exp(-\Delta E_{rev}^{X/Na}F/RT) \quad (A7)$$

From Eqs. (A5) and (A6) it may readily be shown that:

$$(P_X/P_{Na}) = [(P_X/P_{Na})^*(1 + \beta_2)] - \beta_1 \quad (A8)$$

where

$$\beta_2 = (P_{Tris}/P_{Na}) \cdot ([Tris]_i^{Na}/[Na]_i) \quad (A9)$$

$$\beta_1 \equiv (P_{Tris}/P_{Na}) \cdot ([Tris]_i^X/[X]_i) \quad (A10)$$